

Active Fourth-Order Band-Pass RC-filter with Independent Control of Bandwidth and Irregularity of Frequency Response

D.Y. Denisenko
 Information Systems and Radio
 Engineering
 Don State Technical University
 South Russian University
 Rostov-on-Don, Russia
 d.u.denisenko@gmail.com

N.N. Prokopenko
 Information Systems and Radio
 Engineering
 Don State Technical University
 Institute for Design Problems in
 Microelectronics of Russian Academy
 of Sciences
 Rostov-on-Don, Zelenograd, Russia
 prokopenko@sss.ru

N.V. Butyrlagin
 Information Systems and Radio
 Engineering
 Don State Technical University
 Rostov-on-Don, Russia
 nbutyrlagin@mail.ru

Abstract — A new circuit of a fourth-order band-pass RC-filter (BPF) which provides independent adjustment of the main parameters is investigated: the irregularity of frequency characteristic (FC), the bandwidth and the scale transfer coefficient. An algorithm for choosing the circuit parameters to achieve a given accuracy of digital potentiometers is described. The transfer functions of the developed BPF are presented and the frequency response obtained as a result of computer simulation in CAD Micro-Cap is shown.

Keywords — band-pass filter, transfer function, 4th order filter, irregularity of frequency characteristic, bandwidth, gain scale factor, analog-to-digital converter, digital potentiometer.

I. INTRODUCTION

The active band-pass RC-filters (BPF) are one of the important of frequency selection devices (FSD) used, for example, to filter a specific frequency or band of a signal [1-10]. These filter circuits can be designed to accomplish this task by sequentially connecting low-pass (LPF) and high-pass (HPF) filters (Fig. 1) [11].

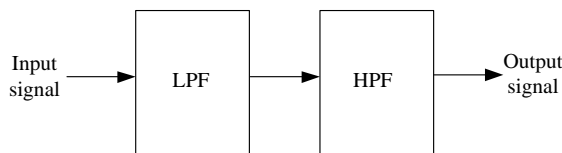


Fig. 1. The block diagram of the classic BPF.

The BPF restructuring can be carried out by changing the nominal values of the frequency setting RC-elements. In practice, varicaps are used as variable capacitors [13-14], but the analog-to-digital converters (ADC) [15] and digital potentiometers (DP) [16-20] are applied as variable resistors.

The can be of different order. The slope of BPF, used in FSD, bind with order and than higher it is, then the more the filter order. In fig. 2 shows the frequency response (FR) for the BPF of the order from 1 to 5 [12].

The purpose and novelty of the article is to develop a fourth-order BPF circuit [21] based on a cascade implementation. The new BPF has the setting of the main parameters - when the bandwidth changes, its transfer coefficient does not change.

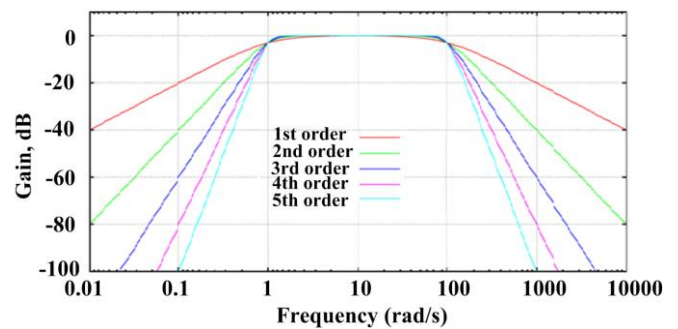


Fig. 2. The BPF of the order from 1 to 5.

II. ANALYSIS OF THE TRANSMISSION FUNCTION OF THE FOURTH ORDER BAND-PASS FILTER

The transfer function of the fourth-order band-pass filter has the form

$$W(p) = M \frac{p^2 b_2^*}{p^4 + p^3 a_3^* + p^2 a_2^* + p a_1^* + a_0^*} \quad (1)$$

where is b_k^*, a_k^* a the coefficients of the numerator and denominator of the transfer function at the corresponding powers p^k .

The BPF is made according to a connected-cascade implementation on identical second-order links with transfer functions of a strip type based on the structures in Fig. 3

$$F_i(p) = K_i \frac{p d_p \omega_p}{p^2 + p d_p \omega_p + \omega_p^2} \quad (2)$$

where is K_i a transfer coefficient of the i-th link.

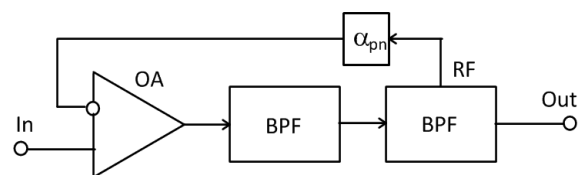


Fig. 3. The BPF structure with an input adder based on operational amplifier (OA).

This work has been supported by the grant the Russian Science Foundation, RSF 18-79-10109.

Transfer function (2) can be represented as

$$W(p) = M \frac{p^2 b_2 \omega_p^2}{p^4 + p^3 a_3 \omega_p + p^2 a_2 \omega_p^2 + p a_1 \omega_p^3 + \omega_p^4}, \quad (3)$$

where is b_k, a_k a the coefficients of the transfer function normalized to the pole frequency; M is a scaled transfer coefficient of the filter.

A change in the relative bandwidth of the fourth-order BPF without changing its other parameters (uneven FR and transfer coefficient) is possible when the damping d_p of one or two links changes, and the K_i coefficients should not change in the links. These conditions correspond to links that have transfer functions with equal coefficients of the polynomials of the numerator and denominator at p. This circumstance is reflected in the formula (2).

Table 1 shows the coefficients of the transfer function (3), expressed through the parameters of the links. In them, the loopback transfer coefficient is denoted by α with indices reflecting the type of connection between the links.

TABLE I. COEFFICIENTS OF THE TRANSFER FUNCTION OF THE BPF, PRESENTED THROUGH THE PARAMETERS OF THE LINKS

Coefficient	Expressions of the coefficients of the transfer functions of the BPF structure
b_2	d_p^2
$a_1 = a_3$	$d_p (2 - \alpha_{pn})$
a_2	$d_p^2 + 2$
M	1

Table 2 summarizes the calculation formulas for determining the maximum value of the frequency response according to the known parameters of the structure, at which it reaches this value, as well as the cutoff frequencies at the level of - 3 dB.

TABLE II. EXPRESSIONS FOR DETERMINING THE MAXIMUM VALUES OF THE FREQUENCY RESPONSE PARAMETERS

Parameter	Frequency response parameter expressions
X_{\max}	$d_p \sqrt{1 - \frac{(2 - \alpha_{pn})^2}{2}}$
A_{\max}	$\frac{2}{(2 - \alpha_{pn}) \sqrt{\alpha_{pn}} \sqrt{4 - \alpha_{pn}}}$
X_{cutoff} (-3 dB)	$d_p \sqrt{\frac{2 - (2 - \alpha_{pn})^2}{2} \pm \sqrt{2 + \frac{1}{4}(2 - \alpha_{pn})^4 - (2 - \alpha_{pn})^2}}$

Having set $X_{\max}=0$, according to the formulas in Table. 2 we find the loopback transfer coefficient is $\alpha_{pn} = 2 - \sqrt{2}$, at which the maximally flat frequency response is realized.

The problem is solved in a fourth-order BPF, where the filter parameters can be found without solving the approximation problem. For the block diagram shown in Fig. 3, α_{pn} is found from the equation

$$\alpha_{pn}^4 - 8\alpha_{pn}^3 + 20\alpha_{pn}^2 - 16\alpha_{pn} + 4/10^{10} = 0, \quad (4)$$

and the damping of the poles is determined by the equation

$$d_p = \frac{X_{cutoff}^{\pm}}{\sqrt{\frac{2 - (2 - \alpha_{pn})^2}{2} \pm \sqrt{2 + \frac{1}{4}(2 - \alpha_{pn})^4 - (2 - \alpha_{pn})^2}}}. \quad (5)$$

In view of the complexity of the solution of equation (5), α_{pn} it is possible to determine in another way - using the relations in Table. 1, we find the parameters $d_p = \sqrt{a_2 - 2}$ and $\alpha_{pn} = 2 - \frac{a_1}{\sqrt{a_2 - 2}}$

shown in Fig. 3.

III. TUNABLE BPF

With a change in the adjustment range and a corresponding decrease in the requirements for the discreteness of the change, determined by the capacity of the DP control code, we can use a circuit based on an operational amplifier (OA) (Fig. 4), and its transfer coefficient is [20]:

$$K(\alpha) = -\frac{R_2}{R_1} \cdot \frac{R_3 + (1 - \alpha)R_1 + \alpha \cdot (1 - \alpha)R}{R_3 + \alpha \cdot R_2 + \alpha \cdot (1 - \alpha)R}, \quad (6)$$

$$0 \leq \alpha \leq 1$$

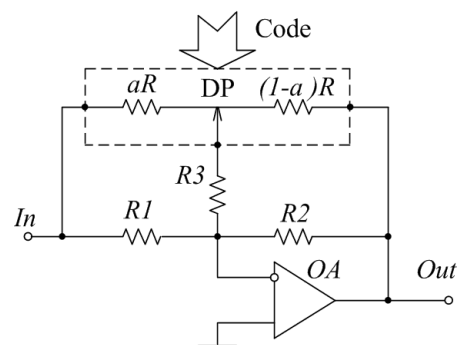


Fig. 4. Amplifier with reduced tuning range.

Increasing the resistance of the resistor will shorten the adjustment range and decrease the variation with change. Thus, the installation accuracy a transfer coefficient of circuit (Fig. 4) is regulated by two parameters - the resistor resistance or the bits of DP. With these two parameters, high accuracy can be achieved with a low bits of DP and low cost.

In [20] the algorithm is described for choosing these parameters to achieve a given accuracy $\delta\%$. Let us supplement the performance with the accuracy $\delta\%$, the requirement for the accuracy of the installation of the transfer coefficient $k\%$ provided by the resistor R_3 . Considering that the dependence is decreasing, to select the resistance R_3 , it is necessary to solve the corresponding system of equations:

$$\begin{cases} K(0) = -\frac{R_2}{R_1} \cdot \frac{R_3 + R_1}{R_3} = -\left(1 + \frac{k}{100\%}\right) \cdot \frac{R_2}{R_1}, \\ K(1) = -\frac{R_2}{R_1} \cdot \frac{R_3}{R_3 + R_2} = -\left(1 - \frac{k}{100\%}\right) \cdot \frac{R_2}{R_1}. \end{cases} \quad (7)$$

The solution to the resulting system (7) has the form:

$$\begin{cases} R_3 = \frac{100\%}{k} \cdot R_1, \\ R_3 = \left(\frac{100\%}{k} - 1\right) \cdot R_2 \end{cases} \quad (8)$$

Since a larger value of R_3 provides a smaller range of change in the transfer coefficient, then for the selected accuracy $k\%$, the resistance of the resistor R_3 is selected according to the following equation

$$R_3 = \max\left(\frac{100\%}{k} R_1, \left(\frac{100\%}{k} - 1\right) R_2\right). \quad (9)$$

The resulting range of change in transfer coefficient

$$\left(1 + \frac{k}{100\%}\right) \cdot \frac{R_2}{R_1} - \left(1 - \frac{k}{100\%}\right) \cdot \frac{R_2}{R_1} = 2 \cdot \frac{k}{100\%} \cdot \frac{R_2}{R_1}, \quad (10)$$

is divided into intervals, the number of which is determined by the capacity of the DP. The more the number of intervals

N , the more accurately the transfer coefficient is set. To ensure the specified accuracy $\delta\%$, the following condition must be met:

$$2 \cdot \frac{k}{100\%} \cdot \frac{R_2}{R_1} \cdot \frac{1}{N} \leq 2 \cdot \frac{\delta}{100\%} \cdot \frac{R_2}{R_1}. \quad (11)$$

From this inequality, the number of intervals necessary to ensure the required accuracy is determined:

$$N \geq \frac{k\%}{\delta\%}. \quad (12)$$

The number of intervals should be selected based on the following considerations:

- $N = 2^n$, where is a n -bits number of DP;
- N should be as small as possible, otherwise excessive accuracy will be required, which will entail unreasonable material costs.

IV. EXAMPLE OF IMPLEMENTATION OF BPF AND RESULTS OF ITS COMPUTER SIMULATION

Fig. 5 show a new BPF [21] based on the structure (Fig. 3) and implemented on OA. Computer simulation of BPF (Fig. 5) was made in the Micro-Cap [22] on models OA OP37C [23] and its schematic diagram shown on Fig. 6.

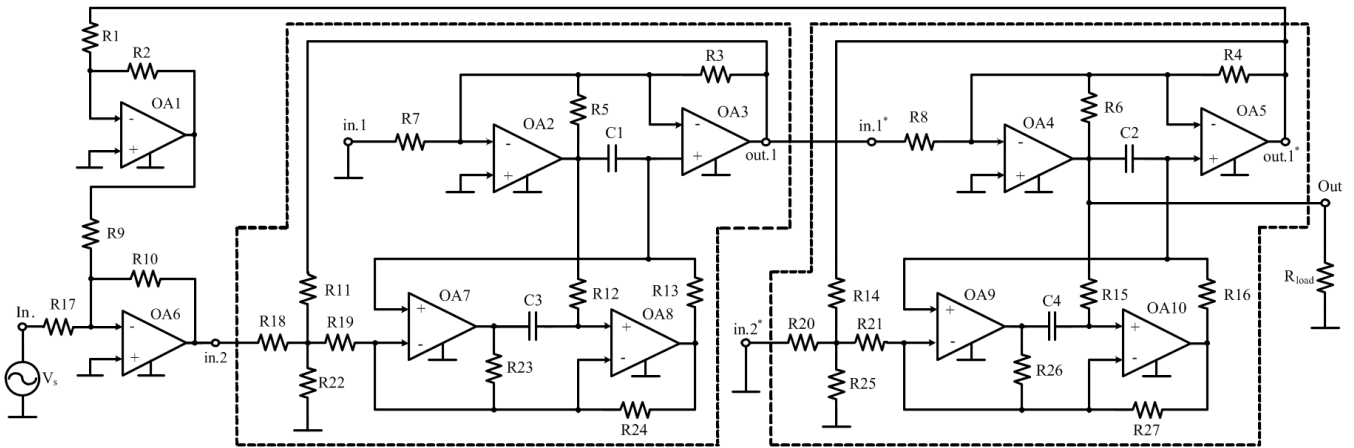


Fig. 5. Schematic diagram of the BPF according to the structure of Fig. 3 [21].

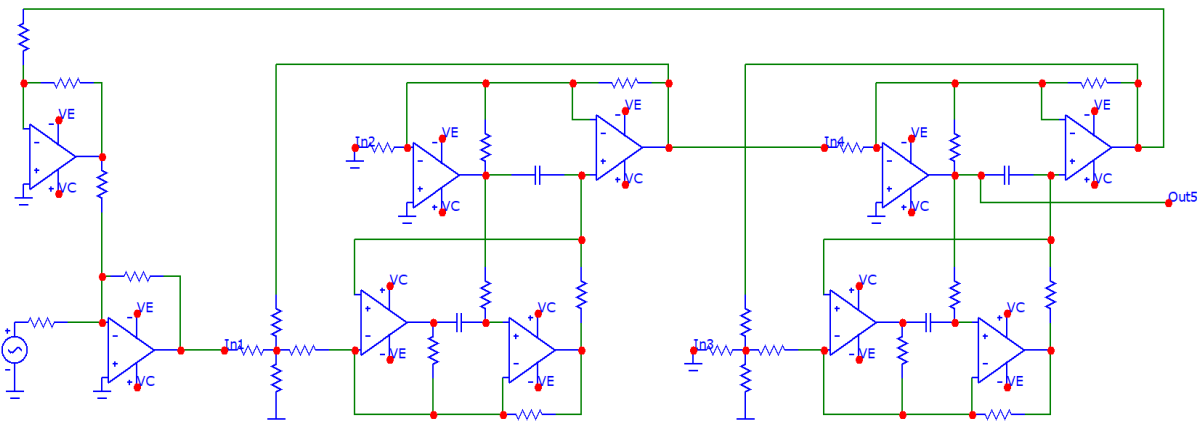


Fig. 6. BPF (Fig. 5) in Micro-Cap CAD.

The results of computer simulation (Fig. 7) show a change in the shape of the FR when adjusting the feedback coefficient without changing the transfer coefficient. This is possible by adjusting the resistance of the resistor R1 in the range from 10 to 40 k Ω .

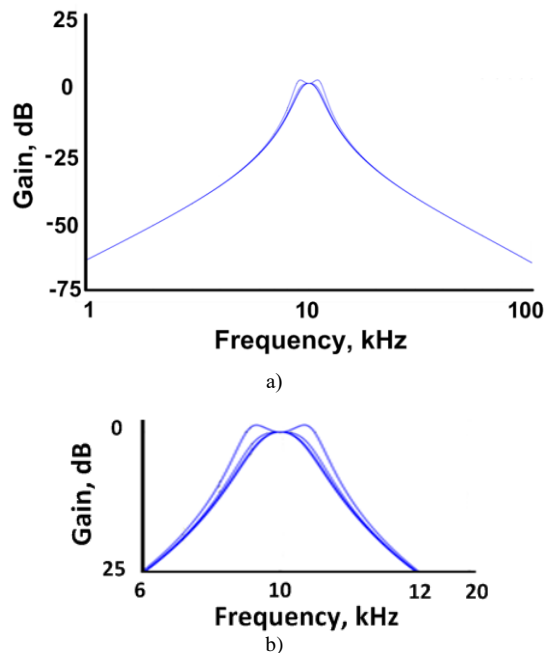


Fig. 7. The FR of a BPF according the circuit Fig. 6 when changing the resistance of R1 (a) and this graphs in big scale (b).

CONCLUSION

A new scheme of the fourth-order BPF based on cascade-connected links has been developed, which has independent adjustment of the main parameters. In the investigated BPF, it is possible to control the bandwidth by changing the attenuation in one or simultaneously in two links. An algorithm for selecting DP parameters to achieve a given accuracy is considered in detail, which can be used in modern FSD.

REFERENCES

- [1] Arthur B. Williams. Analog Filter and Circuit Design Handbook, McGraw-Hill Education: New York, Chicago, San Francisco, Athens, London, Madrid, Mexico City, Milan, New Delhi, Singapore, Sydney, Toronto, March 2014. [Online]. Available: <https://www.accessengineeringlibrary.com/content/book/9780071816717>.
- [2] Analog filters chapter 8, Analog filters, June 2008. [Online]. Available: <https://www.analog.com/media/en/training-seminars/design-handbooks/Basic-Linear-Design/Chapter8.pdf>.
- [3] Lei Zhu, Sheng Sun, Rui Li, Microwave Bandpass Filters for Wideband Communications, Publisher: Wiley, 2012, 240 p.
- [4] R. K. Attri, Narrow Band-Pass Filters for Low Frequency Applications: Evaluation of Eight Electronics Filter Design Topologies, 2019, 104 p.
- [5] S. Yimman, S. Praesomboon, S. Klunium, S. Navarattara and K. Dejhan, "Two-Pole Band-pass Filter Based on All-pass Filter," 2005 5th International Conference on Information Communications & Signal Processing, Bangkok, 2005, pp. 569-573. doi: 10.1109/ICICS.2005.1689111.
- [6] S. Soleimany, M. R. Salehifar and H. Karbalaee, "Designing an active band-pass filter with tunable transversal element at 4-GHz using 0.2 μ m GaAs technology," 2012 6th International Conference on Application of Information and Communication Technologies (AICT), Tbilisi, 2012, pp. 1-5. doi: 10.1109/ICAICT.2012.6398492.

- [7] N. S. Phuoc, "Variable IIR Digital Band-Pass and Band-Stop Filters," 2018 2nd International Conference on Imaging, Signal Processing and Communication (ICISPC), Kuala Lumpur, Malaysia, 2018, pp. 132-137, doi: 10.1109/ICISPC44900.2018.9006707.
- [8] L. Syed, S. H. Hasan, H. Rashid and W. Gulistan, "Designing Band Pass Filter for HF Radio's Front End," 2019 International Conference on Communication Technologies (ComTech), Rawalpindi, Pakistan, 2019, pp. 60-64, doi: 10.1109/COMTECH.2019.8737794.
- [9] W. Ling and C. Kesong, "The Performance Analysis of Second Order Band-pass Filter," 2019 3rd International Conference on Circuits, System and Simulation (ICCS), Nanjing, China, 2019, pp. 41-45, doi: 10.1109/CIRSYSSIM.2019.8935634.
- [10] B. Wu, N. Yuan, F. Zhang and S. Wu, "Wideband band-pass filter with defected ground structure," 2017 IEEE 2nd Advanced Information Technology, Electronic and Automation Control Conference (IAEAC), Chongqing, 2017, pp. 2149-2152, doi: 10.1109/IAEAC.2017.8054397.
- [11] How to Create Band-pass Filter, July 2014. [Online]. Available: <https://www.allaboutcircuits.com/textbook/alternating-current/chpt-8/band-pass-filters/>.
- [12] First and Second Order Low/High/Band-Pass filters, May 2019. [Online]. Available: <http://fourier.eng.hmc.edu/e84/lectures/ActiveFilters/node2.html>.
- [13] R. Chen, Y. Liu, P. Taskas and F. Z. Peng, "Design of control system for solid state variable capacitor with minimum DC capacitor," 2015 IEEE Applied Power Electronics Conference and Exposition (APEC), Charlotte, NC, USA, 2015, pp. 109-114. doi: 10.1109/APEC.2015.7104339.
- [14] A. B. Bhattacharyya and H. Wallinga, "An area-variable MOS varicap and its application in programmable TAP weighting of CCD transversal filters," in IEEE Transactions on Electron Devices, vol. 29, no. 5, pp. 827-833, May 1982. doi: 10.1109/T-ED.1982.20785.
- [15] A. I. Sattarova, V. O. Varlamov and E. M. Lobov, "Design and Simulation of a Hybrid Filter Bank for Processing Wideband Signals with Low-Speed ADCs," 2019 Systems of Signals Generating and Processing in the Field of on Board Communications, Moscow, Russia, 2019, pp. 1-5. doi: 10.1109/SOSG.2019.8706822.
- [16] I. Pandiev, "Analysis and simulation modeling of programmable CFOA-based universal filters with CMOS digital potentiometers," 2017 40th International Spring Seminar on Electronics Technology (ISSE), Sofia, 2017, pp. 1-6, doi: 10.1109/ISSE.2017.8000942.
- [17] E. Lunca, C. Damian, D. Petrisor and O. Postolache, "Programmable active filters based on digital potentiometers," 2012 International Conference and Exposition on Electrical and Power Engineering, Iasi, 2012, pp. 787-791. doi: 10.1109/ICEPE.2012.6463583.
- [18] W. Li, Z. Sha and B. Wang, "The topology and test technology of Digitally Controlled Potentiometers," 2010 International Conference on Machine Learning and Cybernetics, Qingdao, 2010, pp. 2345-2349. doi: 10.1109/ICMLC.2010.5580663.
- [19] B. Ševčík, "Modeling and signal integrity testing of digital potentiometers," Proceedings of the 17th International Conference Mixed Design of Integrated Circuits and Systems - MIXDES 2010, Warsaw, 2010, pp. 570-575.
- [20] D.Yu. Denisenko, Y.I. Ivanov, N.N. Prokopenko, N.A. Dmitrienko, "Digital Potentiometers in the Tasks of Settings Precision Analog RC-filters Taking into Account the Tolerances for Passive Components," 18th IEEE International Conference of Young Specialists on Micro/Nanotechnologies and Electron Devices (EDM2017), June 29 - July 3 2017, pp. 205-210. doi: 10.1109/EDM.2017.7981741.
- [21] D.Yu. Denisenko, N.N. Prokopenko, Yu.I. Ivanov, "Fourth order broadband bandpass filter," RU Patent appl. 2020140330, Filed: February 08, 2021. (In Russian).
- [22] V. Artuhov and O. Brytov, "Digital filter design by Micro-Cap tools," 2015 IEEE 35th International Conference on Electronics and Nanotechnology (ELNANO), Kyiv, Ukraine, 2015, pp. 310-313. doi: 10.1109/ELNANO.2015.7146898.
- [23] OP-37C Datasheet (PDF) - Linear Technology, February 2008. [Online]. Available: <https://www.alldatasheet.com/datasheet-pdf/pdf/70896/LINER/OP-37C.html>.